Radboud Repository

Radboud University Nijmegen

PDF hosted at the Radboud Repository of the Radboud University Nijmegen

The following full text is a preprint version which may differ from the publisher's version.

For additional information about this publication click this link.
http://hdl.handle.net/2066/84402

Please be advised that this information was generated on 2020-11-23 and may be subject to change.

Astronomy & Astrophysics manuscript no. 15092
July 12, 2010
© ESO 2010

arXiv:1007.1536v1 [astro-ph.GA] 9 Jul 2010

LETTER TO THE EDITOR

A HIFI preview of warm molecular gas around χ Cyg : first detection of H_2O emission toward an S-type AGB star ⋆

K. Justtanont[1], L. Decin[2,3], F. L. Schöier[1], M. Maercker[4,22], H. Olofsson[1,5], V. Bujarrabal[6], A.P. Marston[7], D. Teyssier[7], J. Alcolea[8], J. Cernicharo[9], C. Dominik[3,10], A. de Koter[3,11], G. Melnick[12], K. Menten[13], D. Neufeld[14], P. Planesas[6,15], M. Schmidt[16], R. Szczerba[16], R. Waters[3,2], Th. de Graauw[17], N. Whyborn[17], T. Finn[18], F. Helmich[19], O. Siebertz[20], F. Schmülling[20], V. Ossenkopf[20], and R. Lai[21]

(Affiliations can be found after the references)

Received 31 May 2010 / Accepted 9 June 2010

ABSTRACT

Aims. A set of new, sensitive, and spectrally resolved, sub-millimeter line observations are used to probe the warm circumstellar gas around the S-type AGB star χ Cyg. The observed lines involve high rotational quantum numbers, which, combined with previously obtained lower-frequency data, make it possible to study in detail the chemical and physical properties of, essentially, the entire circumstellar envelope of χ Cyg.

Methods. The data were obtained using the HIFI instrument aboard Herschel, whose high spectral resolution provides valuable information about the line profiles. Detailed, non-LTE, radiative transfer modelling, including dust radiative transfer coupled with a dynamical model, has been performed to derive the temperature, density, and velocity structure of the circumstellar envelope.

Results. We report the first detection of circumstellar H_2O rotational emission lines in an S-star. Using the high-J CO lines to derive the parameters for the circumstellar envelope, we modelled both the ortho- and para-H_2O lines. Our modelling results are consistent with the velocity structure expected for a dust-driven wind. The derived total H_2O abundance (relative to H_2) is $(1.1 \pm 0.2) \times 10^{-5}$, much lower than that in O-rich stars. The derived ortho-to-para ratio of 2.1±0.6 is close to the high-temperature equilibrium limit, consistent with H_2O being formed in the photosphere.

Key words. Stars: AGB and post-AGB – Circumstellar matter – Stars: kinematics and dynamics – Stars: individual χ Cyg – Stars: late-type – stars: mass-loss

1. Introduction

Observations of the dust and gas components in the circumstellar envelopes (CSEs) around asymptotic giant branch (AGB) stars have been carried out at different wavelengths. Observations in the infrared trace the dust as well as the warm molecular layer close to the stellar photosphere (e.g., Justtanont et al. 1996; Aoki et al. 1999; Schöier et al. 2002). Submillimeter and radio observations of trace molecules have been used to study the cooler outer parts of the CSEs (e.g., Knapp & Morris 1985; Schöier & Olofsson 2000; Kemper et al. 2003). To bridge this gap, the Infrared Space Observatory (ISO) was used to observe a large number of AGB stars up to almost 200 μm, and in O-rich stars, a number of H_2O emission lines were detected (Barlow et al. 1996; Neufeld et al. 1996). However, the circumstellar far-infrared lines were unresolved. Hence, crucial information about the line profiles remained unknown.

Water is an important molecule in CSEs as it is thought to be one of the main cooling agents in the wind. It is also expected to be a good probe of the inner regions of the CSE where the gas is accelerated. However, to fully explore the potential of H_2O lines as a probe of the circumstellar gas, a full radiative transfer has to be performed. Owing to difficulties in calculating accurate collisional rates coupled with the very high optical depth of the H_2O lines in the inner region of the CSE, slow progress has been made. Nevertheless, calculations of the heating and cooling in the CSEs of O-rich stars suggest that H_2O dominates the cooling in most parts of the envelope until it is photodissociated by interstellar UV photons (Goldreich & Scoville 1976; Justtanont et al. 1994; Maercker et al. 2008, 2009; Decin et al. 2010a), and that some lines should come mainly from the acceleration zone. Eventually, spectrally resolved circumstellar H_2O lines were observed by two space missions dedicated to search for cosmic water line emission: SWAS and Odin. Both missions were able to detect the ground-state line of H_2O at 557 GHz in a number of AGB stars (Harwit & Bergin 2002; Melnick et al. 2001; Justtanont et al. 2005; Hasegawa et al. 2006; Maercker et al. 2009). It was shown that not only the line intensity, but also the line profile is crucial for interpreting the data correctly.

In 2009, the ESA-Herschel Space Observatory (Pilbratt et al. 2010) was launched with the Heterodyne Instrument for the Far-Infrared (HIFI[1], de Graauw et al. 2010), which aims to study H_2O line emission in different environments in our Galaxy and beyond. HIFI offers the opportunity to study the warm molec-

⋆ Herschel is an ESA space observatory with science instruments provided by European-led Principal Investigator consortia and with important participation from NASA.

[1] HIFI has been designed and built by a consortium of institutes and university departments from across Europe, Canada and the United States under the leadership of SRON Netherlands Institute for Space Research, Groningen, The Netherlands and with major contributions from Germany, France and the US. Consortium members are: Canada: CSA, U.Waterloo; France: CESR, LAB, LERMA, IRAM; Germany: KOSMA, MPIfR, MPS; Ireland, NUI Maynooth; Italy: ASI, IFSI-INAF, Osservatorio Astrofisico di Arcetri- INAF; Netherlands: SRON, TUD; Poland: CAMK, CBK; Spain: Observatorio Astronómico Nacional (IGN), Centro de Astrobiología (CSIC-INTA). Sweden: Chalmers University of Technology - MC2, RSS & GARD; Onsala Space Observatory; Swedish National Space Board, Stockholm

Table 1. HIFI observations of χ Cyg.

Molecule	Transition	ν (GHz)	E_{up} (K)	I^a (K km s^{-1})
CO	J=6–5	691.473	116	15.3
CO	J=10–9	1151.985	304	13.6
CO	J=16–15	1841.346	752	13.5
o-H_2O	$1_{10} - 1_{01}$	556.936	61	3.0
p-H_2O	$2_{11} - 2_{02}$	752.033	137	4.2
p-H_2O	$2_{02} - 1_{11}$	987.927	101	7.3
p-H_2O	$1_{11} - 0_{00}$	1113.343	53	8.0
o-H_2O	$3_{12} - 2_{21}$	1153.127	249	7.5
o-H_2O	$3_{21} - 3_{12}$	1162.912	305	1.5
o-H_2O	$3_{03} - 2_{12}$	1716.770	197	18.1

Note to the table: [a]The absolute calibration accuracy is between 10% to 30% (see text).

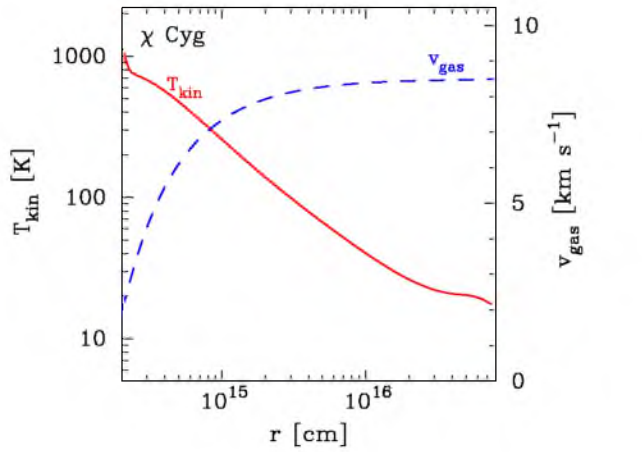

Fig. 1. The derived gas temperature structure (solid line) and the gas expansion velocity (dashed line) of the CSE of χ Cyg.

ular layers in CSEs of AGB stars in great detail, e.g., the high spectral resolution and wide spectral coverage allow a detailed study of the gas dynamics.

As part of the guaranteed time programme HIFISTARS (P.I.: V. Bujarrabal), the S-star (C/O$\approx$1) χ Cyg was selected for study. Distance estimates range from 150 pc (Knapp et al. 2003) to 180 pc (van Leeuwen 2007). The star exhibits SiO masers (e.g., Olofsson et al. 1981; Schwartz et al. 1982; Alcolea & Bujarrabal 1992), but no H_2O maser emission has been found (Menten & Young 1995; Shintani et al. 2008). Being nearby and bright, χ Cyg has been observed using interferometric techniques in both the optical (Lacour et al. 2009) and the infrared (Tevousjan et al. 2004). In this Letter, we briefly describe the observations in Sect. 2, we discuss the modelling of the observed molecular emission in Sect. 3, and present our results and conclusions in Sect. 4.

2. Observations

The HIFI data were obtained using the dual-beam-switching mode (Roelfsema et al. 2010) with a throw of 3′ and slow (0.5-1Hz) chopping in March-April 2010. A total of 8 frequency settings with a total of 10 lines detected are being reported in this paper. The targeted lines were selected to cover a wide range of excitation temperature, exploring different regions of the CSE. As backend, the wide-band spectrometer (WBS) covering a region of 4 GHz with a resolution of 1.1 MHz was used. More details about these observations can be found in Bujarrabal et al. (2010). The data were calibrated using the standard pipeline for Herschel, HIPE version 2.8. Only the H-polarization data are presented here because the V-polarization data are noisier especially for the high frequency lines. We subtracted the baseline using a first or second order polynomial, except for the H_2O transition at 1716 GHz, where this line is affected by standing waves and, consequently, the baseline was fitted using a high order polynomial (see Sect. 3.2).

We detected high rotational transitions of CO as well as the first detection of rotational H_2O in an S-star. All of the observed lines listed in Table 1 were detected. The frequency ν in GHz and the energy of the upper level E_{up} in K are given along with the integrated line intensity, $I = \int T_{mb} d\upsilon$ in K km s^{-1}. The spectra were corrected for the main beam efficiency, i.e., $\eta_{mb} = 0.72 \exp(-(\nu(\mathrm{GHz})/6000)^2)$. The absolute calibration accuracy ranges from 10% for the lowest frequency line to 30% for the high frequency (> 1 THz) lines.

University - Stockholm Observatory; Switzerland: ETH Zurich, FHNW; USA: Caltech, JPL, NHSC.

3. Modelling HIFI lines

We started the analysis by fitting the spectral energy distribution of the CSE (assumed to be spherically symmetric) using Dusty (Ivezic & Elitzur 1997) to derive the dust mass-loss rate. Based on this, we solved the gas-dust drag equation, assuming that both are momentum coupled, to derive the velocity structure using the observed terminal gas velocity as a constraint, as shown in Fig. 3.1. This also provides a so-called dynamical mass-loss rate estimate, 4.9×10^{-7} M$_\odot$ yr^{-1} in the case of χ Cyg (see e.g., Ramstedt et al. 2008). The gas velocity law is fed into the CO radiative transfer model, where the line fluxes and shapes are computed and compared to the observations. At the same time, the heating by dust grains and the cooling by CO lines are calculated and the resulting temperature structure obtained (e.g., Justtanont et al. 1994; Crosas & Menten 1997; Decin et al. 2006; van der Tak et al. 2007; Ramstedt et al. 2008). This provides a circumstellar model, including a mass-loss-rate estimate based on the CO line modelling, which is used to model the H_2O line emission and its contribution to the cooling. The H_2O cooling is then used to recalculate the gas kinetic temperature in the CO model, and the process is iterated until good fits to the observed CO and H_2O lines are obtained.

3.1. Modelling of the CO lines

The Monte Carlo code developed by Schöier & Olofsson (2001) was used to model the observed CO lines. The molecular data were taken from the Hitran database (Rothman et al. 2009) and the collisional rate coefficients from Yang et al. (2010) for the 41 lowest rotational levels in the v = 0 vibrational state. We fitted the line shapes and fluxes for the low-J lines obtained from ground-based observations, as well as the interferometric data for the J = 1–0 and 2–1 lines to more tightly constrain the size of the CO envelope (Schöier et al, in preparation). The parameters are listed in Table 2. The gas kinetic temperature distribution is shown in Fig. 3.1.

We assume a distance of 150 pc (Knapp et al. 2003), and the resulting mass-loss rate is 7×10^{-7} M$_\odot$ yr^{-1} using an adopted CO abundance of 6×10^{-4} (relative to H_2, see Table 2), which provide the best fits to both the line profile and line intensities. The uncertainty in the mass-loss rate is of the order 50%. This mass-loss rate agrees well with the dynamical mass-loss rate (certainly to within the errors in the input parameters). A comparison of the

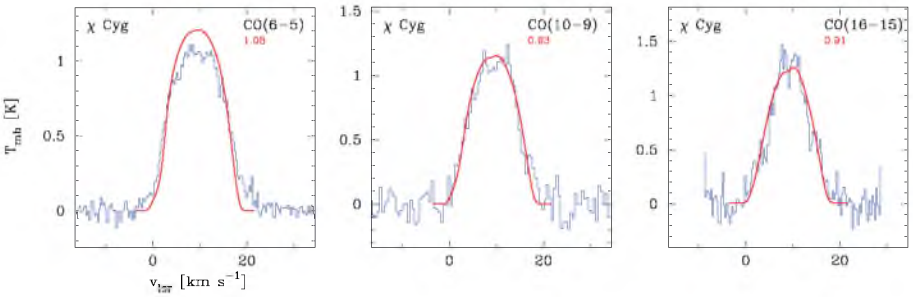

Fig. 2. The model fits (smooth lines) to the HIFI CO $J = 6$–5, 10–9 and 16–15 lines (histogram). The scaling factor (used to scale the model result to fit the observed integrated intensity) is given for each line, showing the goodness of the fit.

Table 2. Parameters used in the modelling of the line emission.

Distance	150 pc
Stellar effective temperature ($T_{\rm eff}$)	2600 K
Stellar luminosity (L_*)	7.5×10^3 $L_\odot$
Gas terminal velocity ($v_{\rm exp}$)	8.5 km s^{-1}
Inner radius of the shell ($R_{\rm in}$)	2×10^{14} cm
Gas mass-loss rate ($\dot{M}$)	7×10^{-7} $M_\odot$ yr^{-1}
CO abundance (CO/H_2)	6×10^{-4}
ortho-H_2O abundance (o-H_2O/H_2)	7.5×10^{-6}
para-H_2O abundance (p-H_2O/H_2)	3.6×10^{-6}

model fits and the HIFI observations can be seen in Fig 2. The models have been scaled to match the line intensities and the scaling factor (given in each panel of the figure) is a measure of the goodness of fit. The high rotational line at $J = 16$–15 is noticeably narrower than the lower-level lines observed with HIFI and ground-based instruments (e.g., Knapp et al. 1998), indicating that this line originates in a region where the gas is still being accelerated. The estimated outer CO radius is 4×10^{16} cm.

3.2. Modelling of the H_2O lines

To calculate the strength and shape of the circumstellar H_2O lines, we apply the parameters derived from our CO line modelling (mass-loss rate, gas temperature and density structure, and gas velocity law) to the radiative transfer model for H_2O based on an accelerated lambda iteration (ALI) code (Justtanont et al. 2005; Maercker et al. 2008, 2009). We used the molecular data from Rothman et al. (2009) and the collisional cross-sections from Faure et al. (2007) for the lowest 45 levels of ortho- and para-H_2O. The radiative excitation due to the absorption in the ν_2 bending and ν_3 stretching modes is included. The latter has been found to have a non-negligible effect in the low mass-loss-rate case (Maercker et al. 2009). The outer radius of the H_2O shell was derived using the model results of Netzer & Knapp (1987), i.e., 3.6×10^{15} cm. Since the ortho- and para-species are expected to be independent, we model the two species separately, using the same circumstellar input values and estimate the two abundances independently. Using the temperature and velocity structure from the CO modelling (Fig 3.1), we calculate the best-fit model to the H_2O lines. All the lines are found to be sub-thermally excited. As mentioned above, both CO and H_2O line cooling is taken into account.

We present the fits to four lines of ortho-H_2O and three lines of para-H_2O observed with HIFI in Fig. 3. These lines span upper energies from 60 to 300 K so the lines probe the cool part of the CSE as well as the warmer inner part. From Figs. 3.1 and 4, it can be seen that H_2O lines originate well within the acceleration zone. All lines are of reasonably high signal-to-noise ratio, including the $3_{03} - 2_{12}$ line, the highest frequency line, where the spectrum is affected by standing waves inside HIFI. For this line, we used a higher order Chebyshev polynomial for the baseline subtraction (bottom right panel of Fig 3).

Our results are consistent with the velocity structure of a dust-driven wind as can be seen in good fits to both the CO and H_2O line profiles (Figs. 2 and 3, respectively). Unlike the case for IK Tau (Decin et al. 2010a,b), no modification to the dynamical calculation is required.

4. Results and conclusions

The observed HIFI lines are reliable probes of the inner CSE as the high-energy lines probe the wind in the acceleration zone. Both the velocity and density structures are tightly constrained using the HIFI lines. The abundance of CO used is 6×10^{-4}, intermediate to those usually adopted for O- and C-rich CSEs. The derived ortho- and para-H_2O abundances are significantly lower, $(7.5\pm1.4) \times 10^{-6}$ and $(3.6\pm0.5) \times 10^{-6}$, respectively (Table 2). These values are well below the limits for O-rich AGB stars of $> 10^{-4}$ (Justtanont et al. 2005; Maercker et al. 2008, 2009) consistent with χ Cyg being an S-star of C/O very close to unity. From our modelling, assuming that all carbon is locked up in CO (i.e., C/H = 3×10^{-4}) and the oxygen is locked up in both CO and H_2O (i.e., O/H = 3×10^{-4} + 5.5×10^{-6}), our derived C/O is ≤ 0.98, given that a small fractional abundance of the oxygen is in dust grains. This value is slightly higher than that of 0.95, assumed by Duari & Hatchell (2000). A non-thermal equilibrium chemistry model for S-stars (C/O = 0.98) predicts an H_2O abundance of 10^{-4} at the stellar photosphere, falling off to a few 10^{-6} at 5 R_* (Cherchneff 2006), an order of magnitude lower than our value.

In the thermal equilibrium (TE) limit at high temperature, the expected ortho-to-para ratio is 3. Our derived ortho-to-para ratio is 2.1±0.6, close to the high-temperature TE value. The reported ortho-to-para ratio in CSEs of O-rich stars vary from 1 in W Hya with a large uncertainty (Barlow et al. 1996) to 3 in IK Tau (Decin et al. 2010b). Our result is consistent with H_2O molecules being formed under thermal equilibrium conditions in the warm and dense stellar photosphere.

Given the low total H_2O abundance of $(1.1 \pm 0.2) \times 10^{-5}$, it is clear from our analysis that the dominating cooling agent in the CSE of χ Cyg is CO (Fig. 4). Vibrationally excited H_2 and rotationally excited H_2O contribute only in the innermost ($r < 10^{15}$ cm) part of the CSE while CO line cooling extends further out until CO is photodissociated by the external UV field. Adiabatic cooling dominates only in the outermost part of the CSE. The derived H_2O abundance, although much lower than in O-rich stars, is higher than that observed in C-stars, IRC+10216 (Melnick et al. 2001) and V Cyg (Neufeld et al. 2010), consistent with AGB stars of S-type being chemically intermediate between O-rich and C-rich AGB stars.

Acknowledgements. HCSS / HSpot / HIPE is a joint development (are joint developments) by the Herschel Science Ground Segment Consortium, consist-

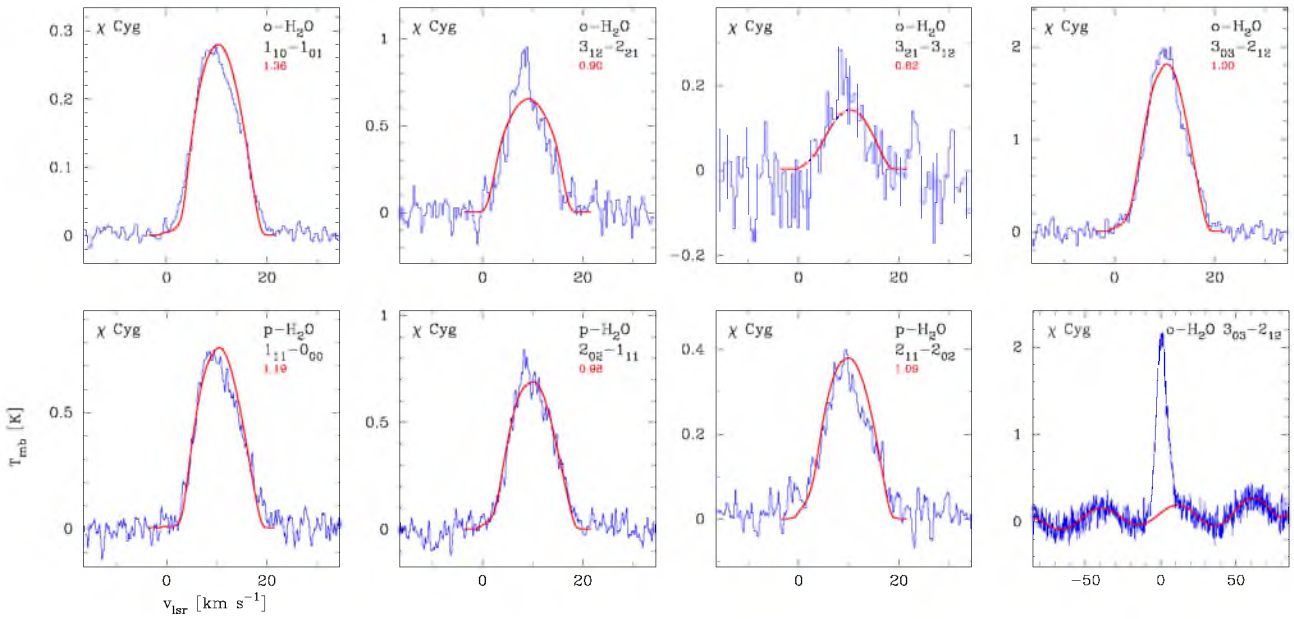

Fig. 3. The model fits (smooth lines) to the HIFI ortho- and para-H_2O lines (histogram). The scaling factor (used to scale the model result to fit the observed integrated intensity) is given for each line, showing the goodness of the fit. The pipeline-reduced data of the $3_{03} - 2_{12}$ line are plotted along with the fitted baseline at the bottom right. This line is affected by standing waves within HIFI.

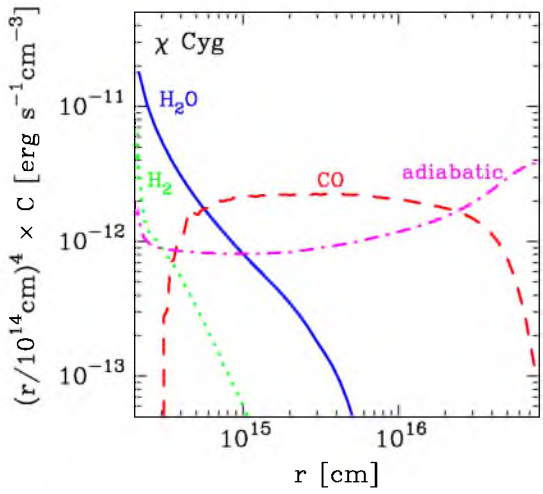

Fig. 4. The cooling rates due to different process : rotational cooling by H_2O (solid), CO (dashed) lines, vibrational cooling by H_2 (dotted) line, and adiabatic cooling (dot-dash).

ing of ESA, the NASA Herschel Science Center, and the HIFI, PACS and SPIRE consortia. K.J., F.S, M.M., and H.O. acknowledge funding from the Swedish National Space Board. This work has been partially supported by the Spanish MICINN, within the program CONSOLIDER INGENIO 2010, under grant "Molecular Astrophysics: The Herschel and Alma Era – ASTROMOL" (ref.: CSD2009-00038). R.Sz. and M.Sch. acknowledge support from grant N 203 393334 from Polish MNiSW. J.C. thanks funding from MICINN, grant AYA2009-07304. This research was performed, in part, through a JPL contract funded by the National Aeronautics and Space Administration.

References

Alcolea, J. & Bujarrabal, V. 1992, A&A, 253, 475
Aoki, W., Tsuji, T., & Ohnaka, K. 1999, A&A, 350, 945
Barlow, M. J., Nguyen-Q-Rieu, Truong-Bach, et al. 1996, A&A, 315, L241
Bujarrabal, V., Alcolea, J., Soria, R., et al. 2010, A&A, this volume
Cherchneff, I. 2006, A&A, 456, 1001
Crosas, M. & Menten, K. M. 1997, ApJ, 483, 913
de Graauw, T., Helmich, F., Phillips, T. G., et al. 2010, A&A, in press
Decin, L., De Beck, E., Brunken, S., et al. 2010a, A&A, in press
Decin, L., Hony, S., de Koter, A., et al. 2006, A&A, 456, 549
Decin, L., Justtanont, K., Waters, L., et al. 2010b, A&A, this volume
Duari, D. & Hatchell, J. 2000, A&A, 358, L25
Faure, A., Crimier, N., Ceccarelli, C., et al. 2007, A&A, 472, 1029
Goldreich, P. & Scoville, N. 1976, ApJ, 205, 144
Harwit, M. & Bergin, E. A. 2002, ApJ, 565, L105
Hasegawa, T. I., Kwok, S., Koning, N., et al. 2006, ApJ, 637, 791
Ivezic, Z. & Elitzur, M. 1997, MNRAS, 287, 799
Justtanont, K., Bergman, P., Larsson, B., et al. 2005, A&A, 439, 627
Justtanont, K., de Jong, T., Helmich, F. P., et al. 1996, A&A, 315, L217
Justtanont, K., Skinner, C. J., & Tielens, A. G. G. M. 1994, ApJ, 435, 852
Kemper, F., Stark, R., Justtanont, K., et al. 2003, A&A, 407, 609
Knapp, G. R. & Morris, M. 1985, ApJ, 292, 640
Knapp, G. R., Pourbaix, D., Platais, I., & Jorissen, A. 2003, A&A, 403, 993
Knapp, G. R., Young, K., Lee, E., & Jorissen, A. 1998, ApJS, 117, 209
Lacour, S., Thiébaut, E., Perrin, G., et al. 2009, ApJ, 707, 632
Maercker, M., Schöier, F. L., Olofsson, H., et al. 2009, A&A, 494, 243
Maercker, M., Schöier, F. L., Olofsson, H., Bergman, P., & Ramstedt, S. 2008, A&A, 479, 779
Melnick, G. J., Neufeld, D. A., Ford, K. E. S., Hollenbach, D. J., & Ashby, M. L. N. 2001, Nature, 412, 160
Menten, K. M. & Young, K. 1995, ApJ, 450, L67+
Netzer, N. & Knapp, G. R. 1987, ApJ, 323, 734
Neufeld, D. A., Chen, W., Melnick, G. J., et al. 1996, A&A, 315, L237
Neufeld, D. A., Gonzalez-Alfonso, E., Melnick, G. A., et al. 2010, A&A, this volume
Olofsson, H., Rydbeck, O. E. H., Lane, A. P., & Predmore, C. R. 1981, ApJ, 247, L81
Pilbratt, G., author2, author3, et al. 2010, A&A, in press
Ramstedt, S., Schöier, F. L., Olofsson, H., & Lundgren, A. A. 2008, A&A, 487, 645
Roelfsema, P., Helmich, F., Teyssier, D., et al. 2010, A&A, this volume
Rothman, L. S., Gordon, I. E., Barbe, A., et al. 2009, J. Quan. Spectroscopy and Radiative Transfer, 110, 533
Schöier, F. L. & Olofsson, H. 2000, A&A, 359, 586
Schöier, F. L. & Olofsson, H. 2001, A&A, 368, 969
Schöier, F. L., Ryde, N., & Olofsson, H. 2002, A&A, 391, 577
Schwartz, P. R., Bologna, J. M., & Zuckerman, B. 1982, ApJ, 256, L55
Shintani, M., Imai, H., Ando, K., et al. 2008, PASJ, 60, 1077
Tevousjan, S., Abdeli, K., Weiner, J., Hale, D. D. S., & Townes, C. H. 2004, ApJ, 611, 466
van der Tak, F. F. S., Black, J. H., Schöier, F. L., Jansen, D. J., & van Dishoeck, E. F. 2007, A&A, 468, 627
van Leeuwen, F. 2007, A&A, 474, 653

Yang, B., Stancil, P. C., Barakrishnan, N., & Forrey, C. 2010, ApJ, submitted

[1] Onsala Space Observatory, Chalmers University of Technology, Dept. Radio & Spece Science, SE–439 92 Onsala, Sweden e-mail: kay.justtanont@chalmers.se
[2] Instituut voor Sterrenkunde, Katholieke Universiteit Leuven, Celestijnenlaan 200D, 3001 Leuven, Belgium
[3] Sterrenkundig Instituut Anton Pannekoek, University of Amsterdam, Science Park 904, NL-1098 Amsterdam, The Netherlands
[4] University of Bonn, Argelander-Institut für Astronomie, Auf dem Hügel 71, D-53121 Bonn, Germany
[5] Department of Astronomy, AlbaNova University Center, Stockholm University, SE–10691 Stockholm, Sweden
[6] Observatorio Astronómico Nacional. Ap 112, E-28803 Alcalá de Henares, Spain
[7] European Space Astronomy Centre, ESA, P.O. Box 78, E-28691 Villanueva de la Cañada, Madrid, Spain
[8] Observatorio Astronómico Nacional (IGN), Alfonso XII N°3, E-28014 Madrid, Spain
[9] CAB, INTA-CSIC, Ctra de Torrejón a Ajalvir, km 4, 28850 Torrejón de Ardoz, Madrid, Spain
[10] Department of Astrophysics/IMAPP, Radboud University Nijmegen, Nijmegen, The Netherlands
[11] Astronomical Institute, Utrecht University, Princetonplein 5, 3584 CC Utrecht, The Netherlands
[12] Harvard-Smithsonian Center for Astrophysics, Cambridge, MA 02138, USA
[13] Max-Planck-Institut für Radioastronomie, Auf dem Hügel 69, D-53121 Bonn, Germany
[14] Johns Hopkins University, Baltimore, MD 21218, USA
[15] Joint ALMA Observatory, El Golf 40, Las Condes, Santiago, Chile
[16] N. Copernicus Astronomical Center, Rabiańska 8, 87-100 Toruń, Poland
[17] Atacama Large Millimeter/Submillimeter Array, Joint ALMA Office, Santiago, Chile
[18] Experimental Physics Dept., National University of Ireland Maynooth, Co. Kildare. Ireland
[19] SRON Netherlands Institute for Space Research, Landleven 12, 9747 AD Groningen, The Netherlands
[20] KOSMA, I. Physik. Institut, Universität zu Köln, Zlpicher Str. 77, D 50937 Köln, Germany
[21] Northrop Grumman Aerospace Systems, 1 Space Park, Redondo Beach, CA 90278 U.S.A
[22] European Southern Observatory, Karl Schwarzschild Str. 2, Garching bei München, Germany